Available online at www.sciencedirect.com
ScienceDirect
Journal of Power Sources 175 (2008) 430–435
JOURNAL OF POWER SOURCES
www.elsevier.com/locate/jpowsour

Short communication

Preparation and performance of nanostructured porous thin cathode for low-temperature solid oxide fuel cells by spin-coating method

Zhicheng Wang, Wenjian Weng *, Kui Chen, Ge Shen, Piyi Du, Gaorong Han

Department of Materials Science and Engineering, Zhejiang University, Hangzhou 310027, China

Received 2 August 2007; received in revised form 22 September 2007; accepted 24 September 2007
Available online 2 October 2007

Abstract

To reduce the cathode–electrolyte interfacial polarization resistance of low-temperature solid oxide fuel cells (SOFCs), a nanostructured porous thin cathode consisting of $Sm_{0.5}Sr_{0.5}CoO_3$ (SSC) and $Ce_{0.8}Sm_{0.2}O_{1.9}$ (SDC) was fabricated on an anode-supported electrolyte film using spin-coating technique. A suspension with nanosized cathode materials, volatilizable solvents and a soluble pore former was developed. The results indicated that the cell with the nanostructured porous thin cathode sintered at 950 °C showed relatively high maximum power density of 212 mW cm^{-2} at 500 °C and 114 mW cm^{-2} at 450 °C, and low interfacial polarization resistance of 0.79 Ω cm^2 at 500 °C and 2.81 Ω cm^2 at 450 °C. Hence, the nanostructured porous thin cathode is expected to be a promising cathode for low-temperature SOFCs.

Keywords: Nanostructured porous thin cathode; Interfacial polarization resistance; Spin coating; Suspension; Low-temperature solid oxide fuel cells

1. Introduction

With the development of the solid oxide fuel cells (SOFCs), more and more attention has been paid on the low working temperature (<600 °C) SOFCs, which demonstrate to be cost-effective, reliable, portable and durable [1–6]. However, operation at low temperature could greatly limit the current output of the SOFCs due to the great increase of cathodic interfacial polarization resistance [7–9]. If such resistance can be decreased, the SOFCs are capable of working well at low temperature.

Two main approaches can be adopted to decrease the cathodic interfacial polarization resistance [7]: (a) changing material compositions or components, such as using mixed ionic/electronic conductor (MIEC) cathode materials [5], and (b) optimizing cathodic structure, such as adjusting porosity, particle size, spatial distribution of electrolyte materials and electrode materials and the cathode thickness [10–14]. It is found that the interfacial polarization resistance could be reduced by creating a nanostructured porous thin electrode with uniform distribution of MIEC [11–12], in which, interconnecting macropores (on the order of micrometers) and nanosized grains are formed. The macropores promote rapidly gas transport through the porous electrodes, and the nanosized grains provide high specific surface areas for gas adsorption/desorption and more catalytically active sites. Furthermore, proper reduction in the thickness of cathode can also decrease polarization resistance because electrochemical reactions can take place throughout the thickness; the thin cathode shows a very low mass transfer resistance [15]. However, till now, how to fabricate such optimal microstructure cost-effectively remains the major technical challenge [11].

Spin coating, as a simple and cost-effective method, has been developed to fabricate porous cathode [16] and thin electrolyte layers [17,18] for SOFC. However, in conventional processes, careful drying and/or baking even sintering processes have to be adopted and repeated for several times [17], leading to non-uniform pores and the grain size, which in turn affects the formation of continuous nanostructured porous structure. In this work, in order to avoid these unfavorable processes and directly obtain nanostructured porous structure, a suspension with nanosized cathode materials, volatile solvents and a soluble pore former was developed. A nanostructured porous thin cathode consisting of SSC (70 wt.%) and SDC (30 wt.%) was prepared on an anode-supported electrolyte film by spin coating. The influence of sintering temperature on the cathodic microstructure and electrochemical properties was studied. Single cell with nanos-

* Corresponding author. Fax: +86 571 87953787.
E-mail address: wengwj@zju.edu.cn (W. Weng).

0378-7753/$ – see front matter © 2007 Elsevier B.V. All rights reserved.
doi:10.1016/j.jpowsour.2007.09.092

tructured porous thin cathode was tested in the temperature range of 450–650 °C.

2. Experimental

2.1. Powder preparation

Nanosized $Ce_{0.8}Sm_{0.2}O_{1.9}$ (SDC) powder, $Sm_{0.5}Sr_{0.5}CoO_3$ (SSC) powder, and NiO–SDC (35 wt.% SDC) powder were prepared by a glycine–nitrate method [19–21]. The stoichiometric amounts of precursors $Ce(NO_3)_4{\cdot}6H_2O$ (99.9%) and $Sm(NO_3)_3{\cdot}6H_2O$ (99.9%) were dissolved in the deioned water. Then, the glycine was added with simultaneous stirring. The molar ratio of NO_3^- to glycine was 2. The resulting solution was heated to evaporate the excess free water until the residual viscous resin transformed into dark-brownish foam. When heated further, spontaneous ignition occurred, and a voluminous, pale-yellow, sponge-like SDC ash was yielded. The SDC ash was subsequently calcined at 700 °C for 2 h to become SDC powder. SSC and NiO–SDC powders were prepared following the similar procedures. SSC powder was mixed with 30 wt.% SDC powder by ball-milling for 72 h. The particle size distribution of ball-milled SDC and SSC powders was measured by Malvern Zeta-Sizer (Nano-S90, Malvern).

2.2. Single cell fabrication

In this work, an anode-supported cell structure was adopted to study the influences of different thin cathodes on the cell performance. Here, the bilayer pieces of anode and electrolyte were prepared using a co-pressing and co-sintering method [8]. The NiO–SDC powders were first pressed at 100 MPa into a disc (∼15 mm diameter and 1 mm thick), then, SDC powder was added onto the disc and co-pressed at 200 MPa to form a bilayer disc. The bilayer disc was co-sintered at 1350 ± 5 °C for 5 h (Nabertherm, Germany). The sintered electrolyte/anode bilayer pieces were used to deposit different cathode to form single cells.

In spin coating for cathode, the suspension consisted of 90 wt.% SSC–SDC powders and 10 wt.% ethylcellulose. The solvent was ethanol and liquid/solid volume ratio was 10. The ethylcellulose was dissolved in ethanol, then the SSC–SDC powder was added, and finally the suspension was homogenized in an airproof vessel by ultrasound for at least 6 h. The suspension was dropped on electrolyte surface of the bilayer pieces, which was immediately spun at 6000 rpm for 30 s to form a uniform layer and remove the solvent at room temperature, and then another cycle was done and 50 cycles were performed of each sample in this work. The samples were fired at 400 °C for 2 h to burn off the ethylcellulose, and then sintered at 900, 950, and 1000 °C in air for 4 h, respectively, to form single cells.

The resulting thin cathodes were characterized by energy dispersive X-ray (EDX) analysis for identifying chemical compositions, and five measurements were made for each sample. The morphologies of the thin cathode were observed using both secondary electron imaging and backscattered electron imaging (BSE) in a field emission scanning electron microscopy (FESEM, Model SIRION-100, FEI). The cathode porosity was obtained from the difference in porosity of the electrolyte/anode bilayer and the single cell, which were characterized by Archimedes' density measurements.

2.3. The performance measurements of the single cells

The single cells were mounted onto a quartz tube. Silver paste was used to seal the anode compartment. A silver current collector was made onto the cathode surface by painting a circular pattern in the center of the cathode using the silver paste [19]. Two silver wires were attached to the anode and cathode with the silver paste. The measurements were conducted from 450 to 650 °C, and the anode and the cathode were fed with humidified (3% H_2O) H_2/air as fuel/oxidant. Current density–voltage (*I–V*) curves of the cells were determined by a potentiostate (CHI600C, CH Instrument) with a constant fuel flow rate of 60 ml min^{-1}. The impedance of the cell was measured in the frequency range from 0.01 Hz to 100 kHz in an ac impedance spectroscopy interfaced with a computer. The microstructure of the post-test single cells was observed by FESEM.

3. Results and discussion

In this work, a single cell consists of ∼20 μm SSC–SDC cathode, ∼25 μm SDC electrolyte and ∼550 μm Ni–SDC anode. Fig. 1a shows its microstructure of a typical post-test single cell. The thin cathode has an interconnected pore structure without large and collapsed pores, and appears to adhere well to the electrolyte. And there are almost no cracks on the surface of cathode as shown in Fig. 1b. The result shows that the porous thin cathode can be directly prepared without any treatment during spin-coating suspension using the developed suspension, and a uniform microstructure is obtained.

3.1. Effect of sintering temperature on microstructure of thin cathode

Fig. 2a–c shows the surface microstructures of the cathode sintered at 900, 950 and 1000 °C, respectively. It is obvious that morphology of the cathode varies depending on sintering temperature. The cathode sintered at 900 °C (Fig. 2(a)) shows smaller grain sizes (25–80 nm) and larger porosity (39%). However, it can be discerned that the primary crystallites agglomerated into larger particles and formed the cathode, which means that the particles in the porous framework have a poor bonding with each other (the inset in Fig. 2(a)). While the cathode sintered at 1000 °C (Fig. 2(c)) shows large size grains (200–500 nm), leading to low specific area of the cathode. Furthermore, the porosity reduces to 25% due to the densification of the ceramics.

When a cathode was sintered at 950 °C, the cathode shows good adhesion to the electrolyte (Fig. 2d). Also the cathode has a good porous structure with the porosity about 31%, and an interconnecting porous structure consisting of well bonded 50–100 nm grains (inset in Fig. 2b). The BSE (Fig. 2e) and EDX analysis results (Fig. 3 and Table 1) demonstrate that nano-

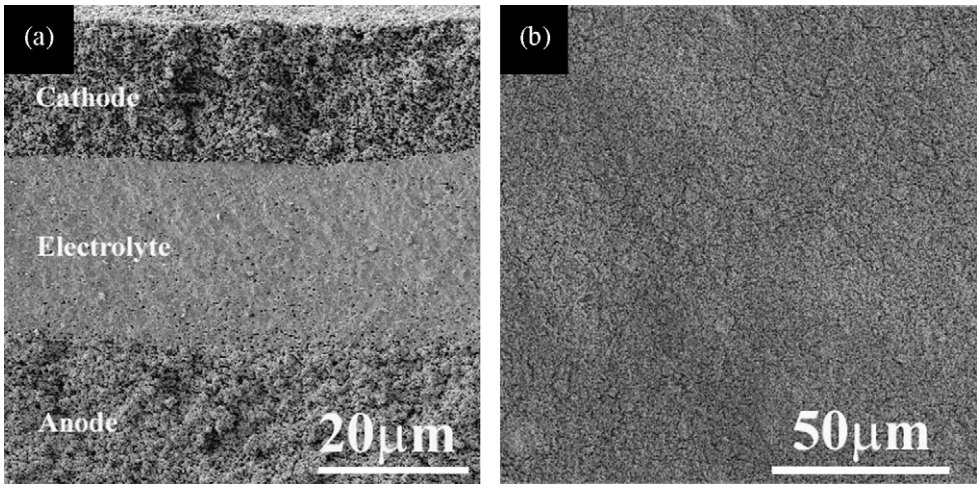

Fig. 1. SEM micrographs of (a) cross-sectional view and (b) surface of the post-test single cell with the cathode sintered at 950 °C.

Table 1
Molar ratio of SSC–SDC thin films deposited by spin coating and after sintering at 950 °C in the air

	Element			
	Sr	Co	Sm	Ce
Observed (%)	17 ± 2	21 ± 2	37 ± 3	25 ± 1
Precursor (%)	17	23	36	24

sized SSC and SDC grains are homogeneously distributed in the framework, and chemical composition is in fairly good agreement with those of the suspension. These indicate a desired nanostructure of a porous cathode can be attained when sintered at 950 °C.

The formation of the nanostructured porous thin cathode could be attributed to that: (1) the nanosized SSC ($d_{50} \sim 167$ nm) and SDC ($d_{50} \sim 44$ nm) powders are mixed well, guaranteeing

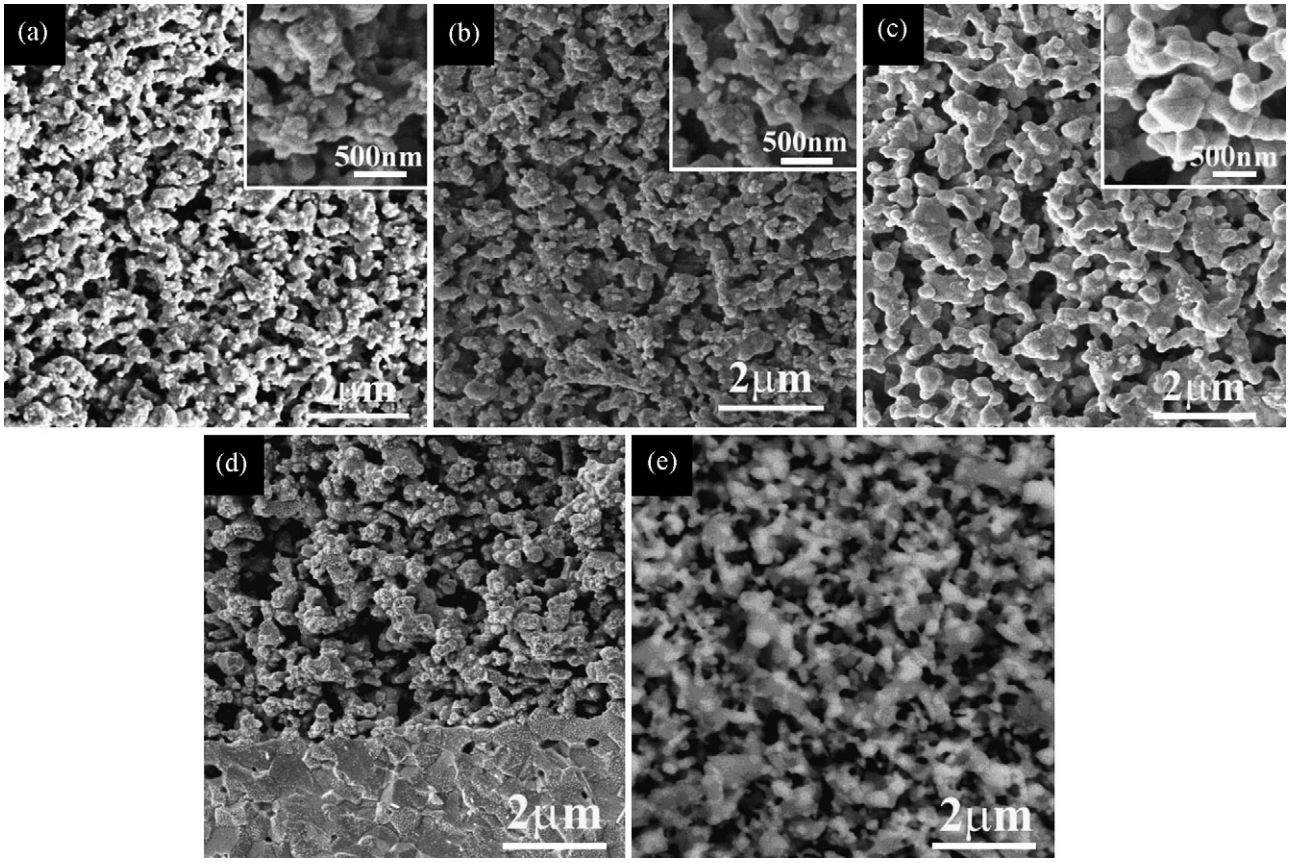

Fig. 2. SEM micrographs of surface microstructures of cathode sintered at 900 °C (a), 950 °C (b) and 1000 °C (c); (d) cross-sectional view of cathode–electrolyte interface and (e) BSE micrograph of cathode sintered at 950 °C.

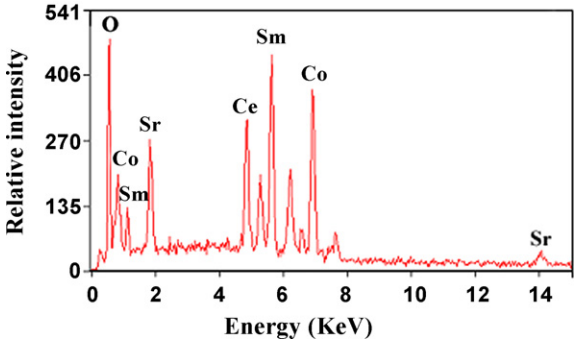

Fig. 3. EDX spectrum of an SSC–SDC layer deposited on the substrate with 6000 rpm and sintered at 950 °C in the air for 4 h. Electron acceleration voltage: 25 kV.

a homogeneous chemical composition distribution and homogeneous microstructure; In addition, uniformly distributed SSC and SDC powders restrains the grain growth each other when the cathode is sintered [22]; (2) the utilization of spin-coating technique and the developed suspension both lead to a porous thin cathode formation; (3) 950 °C sintering of the SSC and SDC particles cause these particles to join together closely but do not grow obviously.

3.2. Effect of different porous cathode on single cell performance

Fig. 4 shows the cell voltages and power densities as functions of current density of cells measured at 600 °C with the cathode sintered at different temperature. Maximum power densities are about 278, 399 and 227 mW cm^{-2}, respectively, when sintered at 900, 950 and 1000 °C.

Fig. 5 shows the electrode impedance spectra measured under open circuit condition for the cathodes sintered at 900, 950 and 1000 °C. Area specific resistance (ASR), a difference in the intercepts on the real axis between high and low frequency, is used to represent the interfacial polarization resistance between electrode and electrolyte [8]. Since the anodes are unchanged in this work, the changes in ASR (Fig. 5) for different single cells could be contributed to the interface between cathode and electrolyte. Therefore, the interfacial polarization resistance of the single cell with the cathode sintered at 950 °C is the lowest.

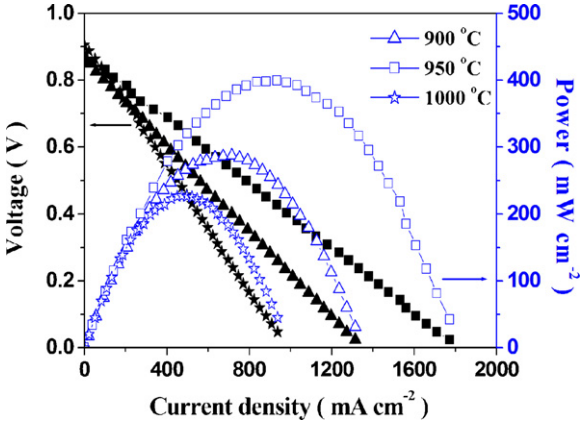

Fig. 4. Cell voltages (solid symbols) and power densities (open symbols) as function of current density of cells tested at 600 °C with the cathode sintered at 900, 950 and 1000 °C.

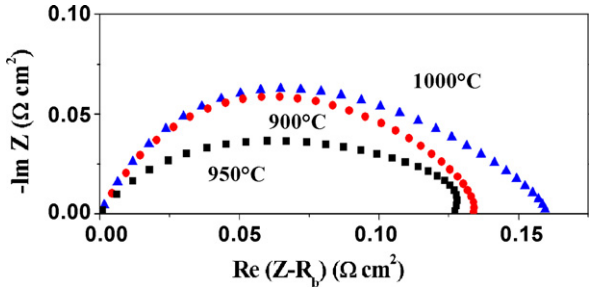

Fig. 5. Electrode impedance spectra measured at 600 °C in open circuit condition for cathodes that sintered at 900, 950 and 1000 °C.

Both the *I–V* curves and impedance spectra show that the single cell with 950 °C sintered cathode obviously has better cell performance than others. This could be attributed to the cell with a required nanostructured porous cathode. In the cathode, the nanosized grains on the cathode framework can provide high surface areas for gas adsorption and desorption, and the uniform distribution of SSC and SDC grains leads to an increase in the active sites for electrochemical reactions for whole cathode. These can strongly favor the electrochemical reactions, and the transportation of electrically charged carriers. As a result, the polarization resistances decrease.

3.3. Performance of the single cell with the nanostructured porous thin cathode

As discussed above, the cell with nanostructured porous thin cathode has preliminarily exhibited good performance at 600 °C. Here, in order to investigate the effects of operation temperature on performances, further electrochemical performances of the cell based on nanostructured porous thin cathode is characterized at 450–650 °C.

AC impedance spectra of the cell under open circuit condition is shown in Fig. 6a using a two-electrode configuration. The ohmic resistances measured from high-frequency intercepts with the real axis are primarily due to contributions from the electrolyte (R_b), and the difference between the intercepts on the real axis at high and low frequency of the impedance loop corresponds to the impedance of the two interfaces [23]: the cathode–electrolyte interface R_c and the anode–electrolyte interface R_a. The total interfacial resistances ($R_a + R_c$) are obtained from the impedance data and open circuit voltage (OCV) measurements [24]. The electrode–electrolyte interfacial polarization resistance is calculated to be 2.81 Ω cm^2 at 450 °C, 0.79 Ω cm^2 at 500 °C, 0.43 Ω cm^2 at 550 °C, 0.17 Ω cm^2 at 600 °C and 0.12 Ω cm^2 at 650 °C, which are shown in Fig. 6b.

It is reported [25] that the resistances of the cathode–electrolyte interface (R_c) are much greater than those of the anode–electrolyte interface (R_a), and the most part of the total interfacial resistances is contributed from the

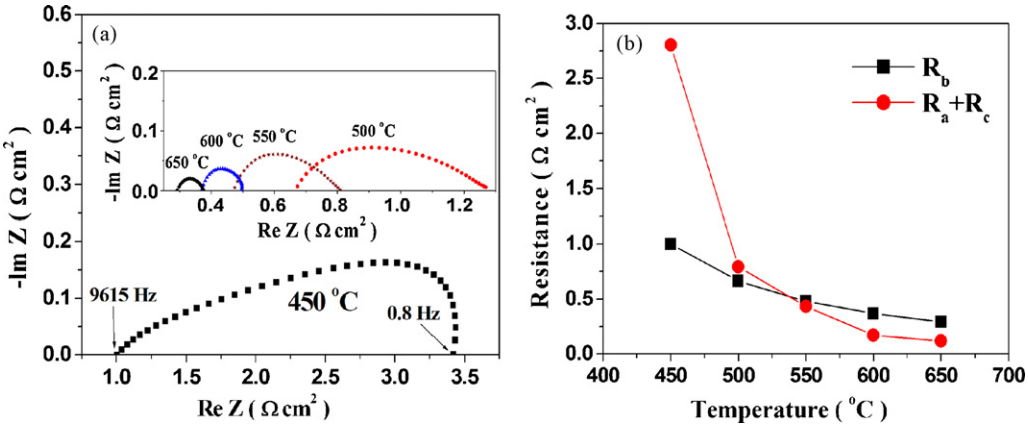

Fig. 6. (a) Impedance spectra of a signal cell measured at 450–650 °C using a two-electrode configuration and (b) the bulk electrolyte (R_b) and total interfacial polarization resistance ($R_a + R_c$) obtained from impedance spectra and OCV.

cathode–electrolyte interfacial polarization. Comparing with other studies [8,11,20] of the cells prepared by the same materials, the obtained interfacial polarization resistance in this work is the lowest, especially when operating temperature is below 550 °C. The total interfacial resistances ($R_a + R_c$) obtained in this study is only 0.79 Ω cm^2, which is less than half of the reported value for a single cell based on a 26 mm thick $Gd_{0.1}Ce_{0.9}O_{1.95}$ electrolyte membrane and an SSC + SDC composite cathode [8].

Fig. 7 shows the cell voltages and power densities as functions of current density and temperature. An OCV of 0.82 V is achieved at 650 °C, which is lower than the theoretical value, that is due to the mixed ionic and electronic conduction of the SDC electrolyte in the reducing environment [26]. With decreasing temperature, the OCV gradually increases to 0.95 V at 450 °C because electronic conductivity in the SDC electrolyte is decreased at low temperatures. Maximum power densities of the cell is operated at 450, 500, 550, 600 and 650 °C are about 114, 212, 293, 399 and 487 mW cm^{-2}, respectively. The cell shows higher maximum power densities than that of the previously reported performance and is about 1.5 times higher than the values reported in Ref. [8] when operation is below

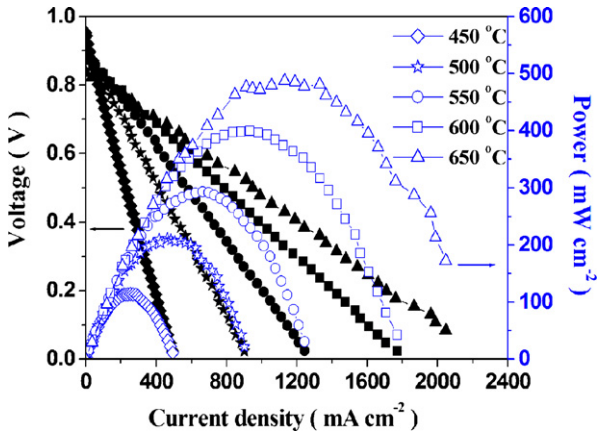

Fig. 7. Cell voltages (solid symbols) and power densities (open symbols) as function of current density of the cell tested at different temperature with the cathode sintered at 950 °C.

550 °C. These indicate again that the performance of SOFC at low temperature can be greatly improved by decreasing the interfacial resistances, while the formation of a nanostructured porous thin cathode is an effective route to reduce the resistance.

4. Conclusions

Nanostructured porous thin cathode consisting of 70 wt.% SSC and 30 wt.% SDC were formed on the anode-supported electrolyte film by spin coating. In the cathode, the nanosized SDC grains distributed uniformly on and across the SSC matrix. The measurements show that the cell with the cathode sintered at 950 °C has the best performance, 212 mW cm^{-2} power density and 0.79 Ω cm^2 interfacial polarization resistance at 500 °C. The good performance is attributed to that the nanostructured porous thin cathode has high triple-phase boundaries (TPBs) length, which favors the electrochemical reactions and the transportation of electrically charged carriers.

References

[1] N.P. Brandon, S. Skinner, B.C.H. Steele, Annu. Rev. Mater. Res. 33 (2003) 183–213.
[2] B.C.H. Steele, A. Heinzel, Nature 414 (2001) 345–352.
[3] Z. Shao, S.M. Haile, Nature 143 (2004) 170–173.
[4] T. Hibino, A. Hashimoto, T. Inoue, J.-I. Tokuno, S.-I. Yoshida, M. Sano, Science 288 (2000) 2031–2033.
[5] C. Xia, M. Liu, Adv. Mater. 14 (2002) 521–523.
[6] S. Piñol, M. Morales, F. Espiell, J. Power Sources 169 (2007) 2–8.
[7] J. Fleig, Annu. Rev. Mater. Res. 33 (2003) 361–382.
[8] C. Xia, M. Liu, Solid State Ionics 144 (2001) 249–255.
[9] J.M. Serra, H.P. Buchkremer, J. Power Sources (2007), doi:10.1016/j.jpowsour.2007.05.018.
[10] D. Beckel, A. Dubach, A.R. Studart, L.J. Gauckler, J. Electroceram. 16 (2006) 221–228.
[11] Y. Liu, S. Zha, M. Liu, Adv. Mater. 16 (2004) 256–260.
[12] J.M. Serra, S. Uhlenbruck, W.A. Meulenberg, H.P. Buchkremer, D. Stöver, Top. Catal. 40 (2006) 123–131.
[13] Y. Liu, C. Compson, M. Liu, J. Power Sources 138 (2004) 194–198.
[14] S.P. Jiang, J. Solid State Electrochem. 11 (2007) 93–102.
[15] M. Ni, M.K.H. Leung, D.Y.C. Leung, J. Power Sources 168 (2007) 369–378.

[16] E. Perry Murray, S.A. Barnett, Solid State Ionics 143 (2001) 265–273.
[17] K. Chen, Z. Lü, N. Ai, X. Huang, Y. Zhang, X. Ge, X. Xin, X. Chen, W. Su, Solid State Ionics 177 (2007) 3455–3460.
[18] N. Ai, Z. Lü, K. Chen, X. Huang, Y. Liu, R. Wang, W. Su, J. Membr. Sci. 286 (2006) 255–259.
[19] C. Xia, W. Rauch, F. Chen, M. Liu, Solid State Ionics 149 (2002) 11–19.
[20] R. Peng, C. Xia, Q. Fu, G. Meng, D. Peng, Mater. Lett. 56 (2002) 1043–1047.
[21] C. Xia, M. Liu, J. Am. Ceram. Soc. 84 (2001) 1903–1905.
[22] X. Zhang, M. Robertson, S. Yick, C. Deĉes-Petit, E. Styles, W. Qu, Y. Xie, R. Hui, J. Roller, O. Kesler, R. Maric, D. Ghosh, J. Power Sources 160 (2006) 1216–1221.
[23] R. Peng, C. Xia, Q. Liu, D. Peng, G. Meng, Solid State Ionics 152–153 (2002) 561–565.
[24] M. Liu, H. Hu, J. Electrochem. Soc. 143 (1996) 109–112.
[25] Y. Wang, H. Nie, S. Wang, T.-L. Wan, U. Guth, V. Valshook, Mater. Lett. 60 (2006) 1174–1178.
[26] T. Matsui, T. Kosaka, M. Inaba, A. Mineshige, Z. Ogumi, Solid State Ionics 176 (2005) 663–668.